2011 American Control Conference
on O'Farrell Street, San Francisco, CA, USA
June 29 - July 01, 2011

LQG Based Robust Tracking Control of Blood Gases during Extracorporeal Membrane Oxygenation

David J. Smith, and Hemanth V. Porumamilla

Abstract – The paper presents three different types of LQG based controllers designed for tracking control of the arterial partial pressures of the blood gases; oxygen and carbon dioxide (O_2 and CO_2) during extracorporeal membrane oxygenation (ECMO). ECMO is a method of support for the heart and or lungs in severely ill patients. In this procedure, the blood is circulated out of the body and into an ECMO machine where the O_2 and CO_2 gas levels are restored before being pumped back into the body. The performance of each of the controllers was ascertained both from a tracking as well as disturbance rejection standpoint to step commands in both these inputs. Robustness analysis was also performed on all the closed loop configurations using the structured singular value analysis. The uncertainty was considered to be of a structured parametric type and was captured by the perturbation of the system "A" matrix. Performance of all the controllers was tuned so as to ensure robust stability to these parametric uncertainties. The LQG and LQG/LTR with feed forward control were able to achieve good tracking performance. But, only the LQG augmented with integral control was able to achieve accurate tracking of the arterial partial pressures of the blood gases in the presence of a step input disturbance in the blood gases flow rates.

I. EXTRACORPOREAL SUPPORT

Extracorporeal support, in general refers to a medical procedure that occurs outside the body, most often applied to circulatory procedures. Examples include hemodialysis, hemofiltration, plasmapheresis, apheresis, extracorporeal membrane oxygenation (ECMO), and cardiopulmonary bypass [2]. This particular study is focused on the use of advanced control methodologies to regulate the arterial partial pressures of O_2 and CO_2 during an ECMO process. ECMO is performed as a method of support for the heart and/or lungs in severely ill patients. In this process, the blood is circulated out of the body and into an ECMO machine where the O_2 and CO_2 gas levels are restored using a membrane oxygenator before being pumped back into the body. This membrane oxygenator performs in a similar function to that of the human lungs by mixing O_2 and CO_2 with the blood. In addition to oxygenating the blood, an ECMO machine maintains the blood temperature at the appropriate level with the help of a heat exchanger such that the body temperature does not drop when the blood is returned, which has serious implications [2]. Additional components of a typical ECMO system include pressure monitors, pump and various drug administration interfaces as shown in Fig. 1.

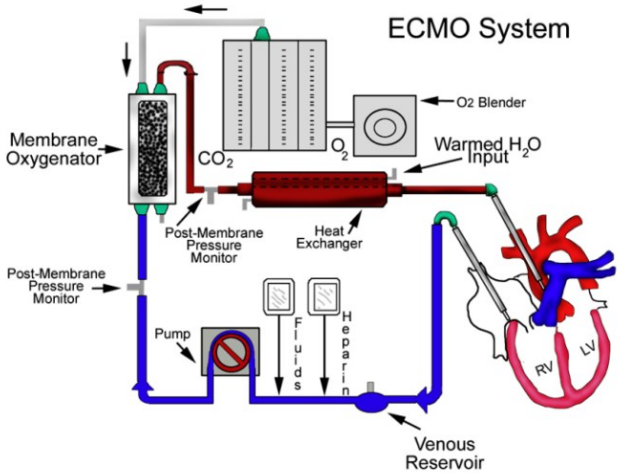

Fig. 1: Typical ECMO hardware setup

II. STATE SPACE MODELING

The main components of a typical ECMO system include a membrane oxygenator, pump, fluids and heparin administration interfaces, heat exchanger, pressure monitor, and blood gas sensors. In this study, only the membrane oxygenator and the blood gas sensors need to be considered for quantifying the system under consideration. As explained earlier, the membrane oxygenator replicates the functionality of the human lungs in that it exposes the blood to regulated amounts of O_2 and CO_2 for assimilation. Firstly, the choice of membrane is critical, since the material should be impermeable to blood, but permeable to O_2 and CO_2 so as to achieve the desired objective [7]. However, the possibility of clots and other obstructions can both impede the functionality of any membrane oxygenator in terms of its mixing capability [8] therby making closed loop control of the device essential. Fig. 2shows a typical membrane oxygenator available in the market and the method by which the O_2 and CO_2 gases are introduced into the oxygenator for mixing.

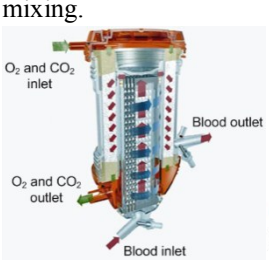

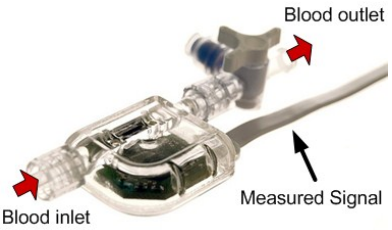

Fig. 2: Membrane blood oxygenator Fig. 3: Arterial blood gas sensor

Manuscript received September 22, 2010.

D. J. Smith is a graduate student of mechanical engineering at Cal Poly State University San Luis Obispo, CA 93407 USA

H. V. Porumamilla is the Chrones assistant professor of mechanical engineering at Cal Poly State University San Luis Obispo, CA 93407 USA (phone: (805) 756-1359 e-mail: hporumam@calpoly.edu)

Owing to new advances in technology, continuous monitoring of blood gases is now possible not only in the form of flow rates of these gases, but also their partial pressures in the blood. This is achieved by the use of a typical blood gas sensor shown in Fig. 3. With this sensor, continuous blood gas monitoring is achieved via a combination of opto-chemical and fiber-optic detectors. These advanced detectors that can measure pH, P_{CO_2}, P_{O_2} and temperature can be inserted in-line with the bloodstream in an artery (8). This component is essential for the modeling of a membrane oxygenator from a controls standpoint, since the amount of O_2 and CO_2 assimilated into the blood is best measured through their arterial partial pressures in the blood. Hence, together with the dynamics of the flow rates of O_2 and CO_2 gases through the membrane oxygenator, and the dynamics of the blood gas sensor that measure the partial pressures of these gases assimilated by blood, the desired state space model of the system under consideration is obtained. One such mathematical model laid out in [1] is used for analysis and control in this paper and is as given below.

$$\dot{x}(t) = \mathbf{A}x(t) + \mathbf{B}_u u(t) + \mathbf{B}_w w(t) \quad (1)$$

$$m(t) = \mathbf{C}_m x(t) + v(t) \quad (2)$$

$$y(t) = \mathbf{C}_y x(t) = \mathbf{C}_m x(t) \quad (3)$$

$$x(t) = [x_1 \quad x_2 \quad x_3 \quad x_4]^T$$

$$u(t) = [u_1 \quad u_2] \quad w(t) = [w_1 \quad w_2] \quad (4)$$

$$\mathbf{A} = \begin{bmatrix} -10 & 0 & 0 & 0 \\ 0 & -10 & 0 & 0 \\ 6 & -3 & -5 & 0 \\ 0 & 0.5 & 0 & -5 \end{bmatrix}; \mathbf{B}_u = \begin{bmatrix} 10 & 0 \\ 0 & 10 \\ 0 & 0 \\ 0 & 0 \end{bmatrix}; \mathbf{B}_w = \begin{bmatrix} 10 & 0 \\ 0 & 10 \\ 0 & 0 \\ 0 & 0 \end{bmatrix}$$

$$\mathbf{C}_m = \begin{bmatrix} 0 & 0 & 1 & 0 \\ 0 & 0 & 0 & 1 \end{bmatrix}$$

$x_1(t)$: flow rate of oxygen; $x_2(t)$: flow rate of carbon dioxide; $x_3(t)$:arterial partial pressure of oxygen (P_{02}); $x_4(t)$: arterial partial pressure of carbon dioxide (P_{C02}); $u_1(t)$:commanded oxygen flow rate; $u_2(t)$: commanded carbon dioxide flow rate; $w_1(t)$: error in the oxygen valve position; $w_2(t)$: error in the carbon dioxide valve position.

III. CONTROLLER DESIGN

In this study, several H_2 linear optimal control techniques based on the Linear Quadratic Gaussian (LQG) control formulation were designed and simulated. The LQG control system design which is based on the use of a stochastic linear quadratic regulator in cascade with a Kalman filter aims at minimizing a quadratic cost function involving selected states and inputs of the system. The original LQG formulation is such that it functions as a regulator (all states are driven to zero). In order to be able to track a non-zero reference, the LQG control methodology was modified in two ways.

A. LQG and LQG/LTR with Feedforward Control

As shown in Fig. 4, in order to incorporate feedforward control, a feedforward control gain (K_r) is added to the above expression. The new control input to the plant is now given by

$$u(t) = -\mathbf{K}\hat{x}(t) + \mathbf{K}_r r(t);\ \mathbf{K}_r = -\{\mathbf{C}_y(\mathbf{A} - \mathbf{B}_u\mathbf{K})^{-1}\mathbf{B}_u\}^{-1} \quad (5)$$

This feedforward control gain can be selected to drive the performance outputs to the desired values after first generating the Linear Quadratic Regulator feedback gains (K) and then obtaining the value for the gain K_r. Using the plant dynamics given by (1)-(3) and the LQG with feedforward control law given by (6), the closed loop system equations can be obtained and are as shown below.

$$\begin{bmatrix} \dot{x}(t) \\ \dot{e}(t) \end{bmatrix} = \begin{bmatrix} \mathbf{A} - \mathbf{B}_u\mathbf{K}(t) & \mathbf{0} \\ \mathbf{0} & \mathbf{A} - \mathbf{G}\mathbf{C}_m \end{bmatrix} \begin{bmatrix} x(t) \\ e(t) \end{bmatrix} + \begin{bmatrix} \mathbf{B}_w & \mathbf{0} & \mathbf{B}_u\mathbf{K}_r \\ \mathbf{B}_w & -\mathbf{G} & \mathbf{0} \end{bmatrix} \begin{bmatrix} w(t) \\ v(t) \\ r(t) \end{bmatrix} \quad (6)$$

$$y(t) = [\mathbf{C}_y \quad \mathbf{0}] \begin{bmatrix} x(t) \\ e(t) \end{bmatrix} \quad (7)$$

As is common knowledge, the basic LQG control scheme loses much of the robustness to modeling and other uncertainty that is provided by the LQR control methodology. Using a technique called Loop Transfer Recovery (LTR), it has been noticed that some of this robustness could be recovered. LTR achieves this objective by adding a fictitious noise input to the control input during Kalman Filter design, which has the effect of reducing the filter's reliance on the control input and also making it faster at the same time. This results in the estimated states reaching the actual states quicker, thereby making the closed loop appear more like that of the LQR. For comparison, an LQG/LTR controller design was also undertaken in this study. The new state equation for the plant dynamics in the case of the LQG/LTR controller becomes

$$\dot{x}(t) = \mathbf{A}x(t) + \mathbf{B}_u u(t) + [\mathbf{B}_w \quad \mathbf{B}_u] \begin{bmatrix} w(t) \\ w_f(t) \end{bmatrix} \quad (8)$$

And the new spectral density matrix is given by,

$$\mathbf{S}_{\begin{bmatrix} w \\ w_f \end{bmatrix}} = \begin{bmatrix} \mathbf{S}_w & \mathbf{0} \\ \mathbf{0} & S_{wf}\mathbf{I} \end{bmatrix} \quad (9)$$

The closed loop system then becomes

$$\begin{bmatrix} \dot{x}(t) \\ \dot{e}(t) \end{bmatrix} = \begin{bmatrix} \mathbf{A} - \mathbf{B}_u\mathbf{K} & \mathbf{0} \\ \mathbf{0} & \mathbf{A} - \mathbf{G}\mathbf{C}_m \end{bmatrix} \begin{bmatrix} x(t) \\ e(t) \end{bmatrix} + \begin{bmatrix} \mathbf{B}_w & \mathbf{B}_u & \mathbf{0} & \mathbf{B}_u\mathbf{K}_r \\ \mathbf{B}_w & \mathbf{0} & -\mathbf{G} & \mathbf{0} \end{bmatrix} [w(t) \quad w_f(t) \quad v(t) \quad r(t)]^T \quad (10)$$

In this study, the LQG and LQG/LTR, both modified by feedforward control were designed and analyzed from a performance as well as robustness standpoint. A schematic of the closed loop system with these two controller configurations is shown in Fig. 4. The results of the simulation are presented in Sec. IV.

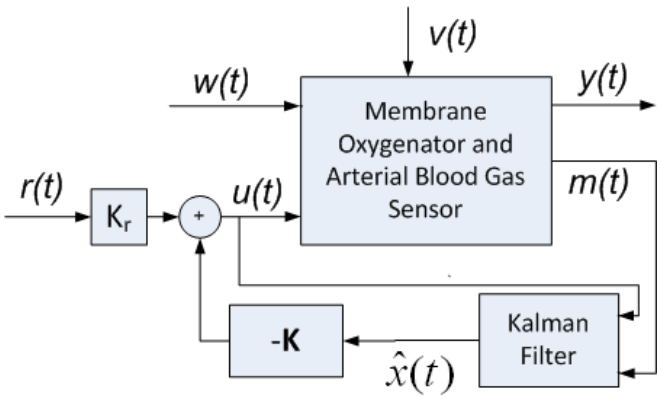

Fig. 4: LQG and LQG/LTR with Feedforward control

B. *LQG Augmented with Integral Action*

Although the LQG methodology works well for white noise inputs, the controller does not increase the system type. If the plant being controlled intrinsically does not have an integrator, the closed loop system with the basic LQG controller even with the feedforward modification cannot achieve good performance to inputs of a higher type such as a step input. Hence, to achieve good tracking and disturbance rejection to step inputs, the LQG controller has to be augmented with integral action. In this study, one such LQG controller augmented with integral action is designed, and is compared to the above mentioned two LQG variants from a performance and robustness standpoint. A schematic of the LQG control scheme augmented with integral action is shown in Fig. (5).

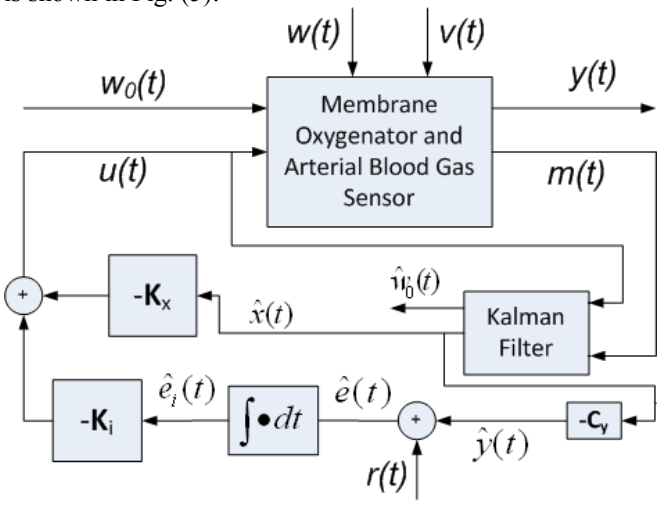

Fig. 5: LQG augmented with integral control

Unlike the basic LQG methodology, the Kalman filter in the integral control system estimates both the plant state and the disturbance input. In order to accomplish this objective, a second disturbance input w_0(t) has to be augmented to the white noise disturbance input w(t) in (1), as described by the method in [1]. This disturbance input, w_0(t), which is of the step input type, is considered to be defined by (13).

$$\dot{w}_0(t) = w_T(t) \tag{11}$$

where, w_o(t) is the disturbance input now considered to be the augmented system state and w_T(t) is the white noise that drives it. In order to account for the additional integral action, (1) has to be augmented with (13). These new augmented system equations given by (14) and (15) are used for finding the Kalman gains.

$$\begin{bmatrix}\dot{x}(t)\\ \dot{w}_0(t)\end{bmatrix} = \underbrace{\begin{bmatrix}\mathbf{A} & \mathbf{B}_{w_0}\\ \mathbf{0} & \mathbf{0}\end{bmatrix}}_{A_f}\begin{bmatrix}x(t)\\ w_0(t)\end{bmatrix} + \underbrace{\begin{bmatrix}\mathbf{B}_u\\ \mathbf{0}\end{bmatrix}}_{B_{uf}}u(t)$$
$$+ \underbrace{\begin{bmatrix}\mathbf{B}_w & \mathbf{0}\\ \mathbf{0} & \mathbf{I}\end{bmatrix}}_{B_{wf}}\underbrace{\begin{bmatrix}w(t)\\ w_T(t)\end{bmatrix}}_{w_d}; B_{w_0} = [\mathbf{I} \quad 0]^T$$

$$\left(\dot{x}_f(t) = A_f\, x_f(t) + B_{u_f}u(t) + B_{w_f}w_d(t)\right) \tag{12}$$

$$m(t) = \underbrace{[\mathbf{C}_m \quad 0]}_{C_f}\begin{bmatrix}x(t)\\ w_0(t)\end{bmatrix} + v(t); y_f(t) = C_f x_f(t) + v(t) \tag{13}$$

In order to generate the control, the LQR gains need to be computed. This also requires the knowledge of the integration action, since the feedback gains must include a separate gain for the integral controller. Hence, the augmented plant must now include the integral error state equation as well. As can be seen from the schematic, the error state equation is defined as,

$$\hat{e}_I = \int \hat{e}\, dt \;\rightarrow\; \hat{e}_I = \int\left(-\mathbf{C}_y\hat{x} + r(t)\right)dt \tag{14}$$

By differentiating the above equation we get the governing error state equation to be,

$$\dot{\hat{e}}_I = -\mathbf{C}_y\hat{x} + r(t) \tag{15}$$

Hence the new augmented plant equation for computing the LQR gains is given by the equations (18) and (19).

$$\begin{bmatrix}\dot{\hat{x}}(t)\\ \dot{\hat{w}}_0(t)\\ \dot{\hat{e}}_I(t)\end{bmatrix} = \underbrace{\begin{bmatrix}\mathbf{A}_f - \mathbf{B}_{uf}[\mathbf{K}_x \quad 0] - \mathbf{G}\mathbf{C}_{mf} & -\mathbf{B}_{uf}K_I\\ -[\mathbf{C}_y \quad 0] & 0\end{bmatrix}}_{A_c}\begin{bmatrix}\hat{x}(t)\\ \hat{w}_0(t)\\ \hat{e}(t)\end{bmatrix}$$
$$+ \underbrace{\begin{bmatrix}\mathbf{G}\\ 0\end{bmatrix}}_{B_c}m(t) + \underbrace{\begin{bmatrix}0\\ 0\\ \mathbf{I}\end{bmatrix}}_{B_r}r(t)$$

$$(\dot{x}_c(t) = A_c\, x_c(t) + B_c\, m(t) + B_r r(t)) \tag{16}$$

$$u(t) = \underbrace{[\mathbf{K}_x \quad 0 \quad \mathbf{K}_I]}_{C_c}\begin{bmatrix}\hat{x}(t)\\ \hat{w}_0(t)\\ \hat{e}_I(t)\end{bmatrix}; (y_c(t) = C_c x_c(t)) \tag{17}$$

Hence the closed loop system is given by,

$$\begin{bmatrix}\dot{x}(t)\\ \dot{x}_c(t)\end{bmatrix}=\begin{bmatrix}\mathbf{A} & \mathbf{B}_u\,\mathbf{C}_c\\ \mathbf{B}_c\,\mathbf{C}_m & \mathbf{A}_c\end{bmatrix}\begin{bmatrix}x(t)\\ x_c(t)\end{bmatrix}+$$

$$\begin{bmatrix}\mathbf{B}_w & 0 & \mathbf{B}_{w_0} & 0\\ 0 & \mathbf{B}_c & 0 & \mathbf{B}_r\end{bmatrix}\begin{bmatrix}w(t)\\ v(t)\\ w_0(t)\\ r(t)\end{bmatrix} \quad (18)$$

$$y(t)=\begin{bmatrix}\mathbf{C}_y & 0\\ 0 & \mathbf{C}_c\end{bmatrix}\begin{bmatrix}x(t)\\ x_c(t)\end{bmatrix} \quad (19)$$

IV. Uncertainty Analysis

Uncertainty analysis is a critical aspect that has to be considered whenever mathematical modeling is performed to capture the dynamics of a real-world system. For the analytical modeling of the extracorporeal membrane oxygenation procedure, the uncertainty is assumed to be structured and of a parametric type affecting the values in the system "A" matrix as shown by (22).

$$\begin{bmatrix}-10 & 0 & 0 & 0\\ 0 & -10 & 0 & 0\\ k_1 & -k_2 & -5 & 0\\ 0 & k_3 & 0 & -5\end{bmatrix} \quad (20)$$

Where the parametric values k_1, k_2, and k_3 are uncertain but bounded in the range $k_1 \in [4,8]$; $k_2 \in [2,4]$; $k_3 \in [0.1,0.9]$. Comparing (1) with (23), it can be noticed that the mean values of the uncertainty range is chosen for the nominal plant dynamics. The stability of a system to a structured uncertainty is determined by analyzing the feedback system shown in Fig. 6 and Fig. 7. Since the nominal closed-loop system is assumed to be stable, any unstable poles of this system are therefore caused by closing the loop through the perturbation (Δ). It can be shown that the feedback system in Fig. 6 and Fig. 7 are internally stable for all possible perturbations if the magnitude of the structured singular value (SSV) of the transfer matrix seen by the Δ over the entire range of desired frequencies is less than or equal to one. This condition is mathematically stated in (24).

$$sup_{\omega}\{\mu_{\bar{\Delta}}[\mathbf{N}_{y_d w_d}(j\omega)]\} < 1 \forall \Delta(j\omega) \in \bar{\Delta};\ \|\Delta(j\omega)\|_{\omega} \le 1 \quad (21)$$

$N_{y_d w_d}$ (the transfer matrix seen by the Δ) is nothing but the transfer matrix within the dotted box (Fig. 6 and Fig. 7). The procedure to find this transfer function matrix is covered in detail in [1]. For the configuration shown in Fig. 6, the corresponding transfer matrix for the SSV analysis is given by (25).

$$N_{y_d w_d}(j\omega) = \mathbf{M}[s\mathbf{I}-\mathbf{A}+\mathbf{G}\mathbf{C}_m(s\mathbf{I}-\mathbf{A}+\mathbf{B}_u\mathbf{K}-\mathbf{G}\mathbf{C}_m)\mathbf{B}_u\mathbf{K}]^{-1} \quad (22)$$

For the case of LQG with integral action shown in Fig. 7, the corresponding transfer matrix for the SSV analysis is given by (26).

$$N_{y_d w_d}(j\omega) = \mathbf{M}[s\mathbf{I}-\mathbf{A}+\mathbf{G}\mathbf{C}_m(s\mathbf{I}-\mathbf{A}+\mathbf{P}-\mathbf{G}\mathbf{C}_m)\mathbf{B}_u\mathbf{K}]^{-1};\ \mathbf{P}=\mathbf{B}_u[s\mathbf{I}[s\mathbf{I}-\mathbf{K}_i\mathbf{K}_x\mathbf{C}_m]^{-1}\mathbf{K}_x] \quad (23)$$

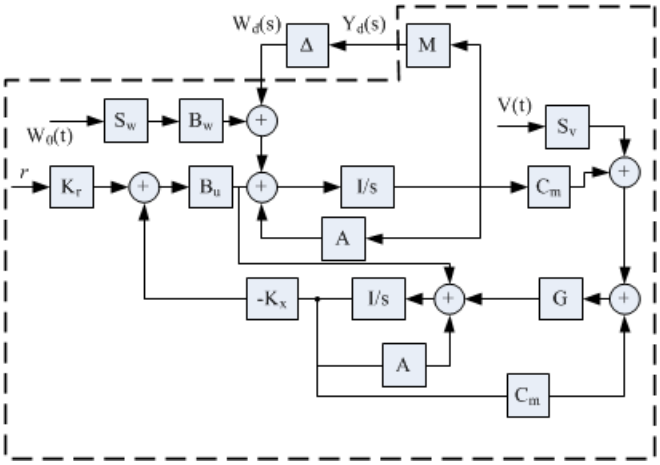

Fig. 6: Structured uncertainty block diagram (LQG and LQG/LTR)

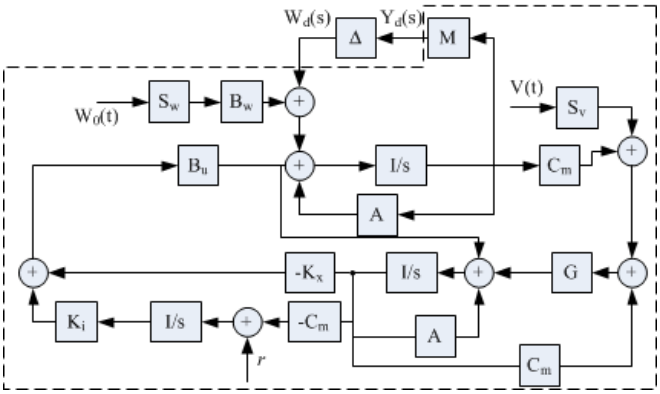

Fig. 7: Structured uncertainty block diagram (LQG with integral action)

V. Results

The main objective of control design for an ECMO process was to accurately track the arterial partial pressures of O_2 and CO_2 in the blood by regulating the flow rates of the gases. To ascertain the tracking performance, the closed loop systems were subjected to step reference inputs in the partial pressures of both these gases, (27).

$$\begin{bmatrix}r_1\\ r_2\end{bmatrix}=\begin{bmatrix}50\\ 5\end{bmatrix}\begin{matrix}\rightarrow P_{O_2}\\ \rightarrow P_{CO_2}\end{matrix} \quad (24); \qquad \begin{bmatrix}w_1\\ w_2\end{bmatrix}=\begin{bmatrix}-20\\ 2\end{bmatrix}\begin{matrix}\rightarrow P_{O_2}\\ \rightarrow P_{CO_2}\end{matrix} \quad (25)$$

To further ascertain the tracking performance of the different controllers in the presence of disturbances, step inputs in disturbance, with a magnitude of 40% that of the reference, were applied after steady state values were reached for the tracking reference input. A step disturbance input, as given in (2), was applied to the system. This step change in in disturbance could be thought of as an error in the flow rate valve position that might be caused due to nonlinear actuator dynamics in the form of sudden jerks. An extreme case of disturbance where the oxygen flow rate was reduced and at the same time, the carbon dioxide flow rate was increased was simulated. With the above mentioned parametric values for the reference and disturbance inputs, the three different controllers were synthesized for optimal tracking and disturbance rejection performance while providing robust stability to the parametric uncertainty described in the

previous section. The various gains and design parameters resulting for the different controllers are given below.
The design parameters shown in Table 1 were identical for the three different controllers.

Table 1

$$Q = \begin{bmatrix} 0 & 0 & 0 & 0 \\ 0 & 0 & 0 & 0 \\ 0 & 0 & 1 & 0 \\ 0 & 0 & 0 & 1 \end{bmatrix} \qquad S_w = \begin{bmatrix} 0.02 & 0 \\ 0 & 0.01 \end{bmatrix}$$

$$S_v = \begin{bmatrix} 1 \times 10^{-4} & 0 \\ 0 & 1 \times 10^{-5} \end{bmatrix}$$

$$R = \begin{bmatrix} 0.1 & 0 \\ 0 & 0.1 \end{bmatrix} \qquad W_{e_i} = \begin{bmatrix} 10 & 0 \\ 0 & 100 \end{bmatrix}$$

Table 2 shows a comparison of the different controller gains for the corresponding controllers.

Table 2

	LQG		LQG/LTR		LQG+Integral	
K^T	0.70	-0.34	0.70	-0.34	0.96	-0.37
	-0.34	0.19	-0.34	0.19	-0.37	0.42
	1.66	-0.82	1.66	-0.82	2.48	-1.06
	0.08	0.29	0.08	0.29	2.24	5.27
K_r^T	3.08	-1.11	3.08	-1.11	-	-
	5.12	10.43	5.12	10.43	-	-
G	83.82	33.02	783.7	756.8	84.2	33.84
	-19.58	98.67	-325.5	2056	-19.70	100.7
	28.86	-4.36	101.5	-21.50	28.93	-4.39
	-0.44	6.03	-2.10	40.10	-0.44	6.13
K_i	-	-	-	-	-9.24	3.81
	-	-	-	-	-12.06	-29.23

Step response analysis was carried out with the above mentioned parametric values obtained from the synthesis of the controllers. Fig. 8 and Fig. 9 show the step response of the arterial partial pressures of O_2 and CO_2 respectively. It can be clearly seen that while all the controllers provide excellent tracking performance to the reference input, only the LQG controller augmented with integral action is able to totally reject a step input in disturbance given in (28) that was applied to the system at 2.5 s. The ability to reject disturbance is as critical as tracking, since, as already mentioned, variation in blood gas levels over a prolonged time can result in life threatening consequences. Also, it can be noticed that although the LQG augmented with integral control provides slower response than the other two controllers, its well within the accepted limits (≈ 30 sec).

Fig. 10 and Fig. 11 show the control inputs provided by the different controllers in the form of flow rates of O_2 and CO_2 gases. Using the rise time criteria, a rough idea of the actuator bandwidth can be calculated for the different controllers. Table (3) provides the corresponding parameters.

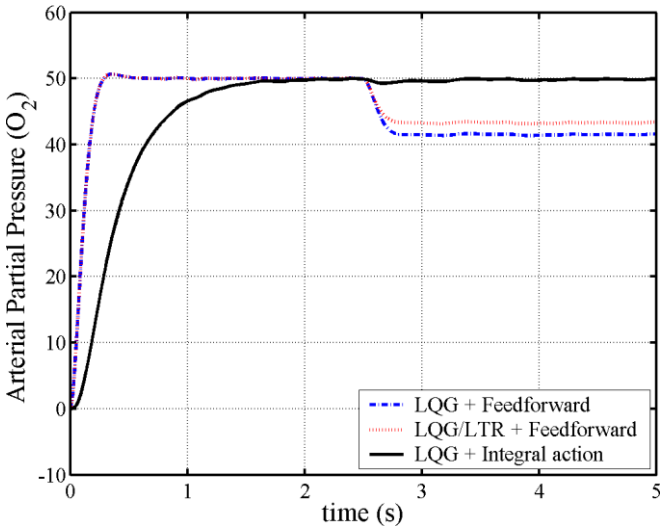

Fig. 8: Step response of O_2 arterial partial pressure

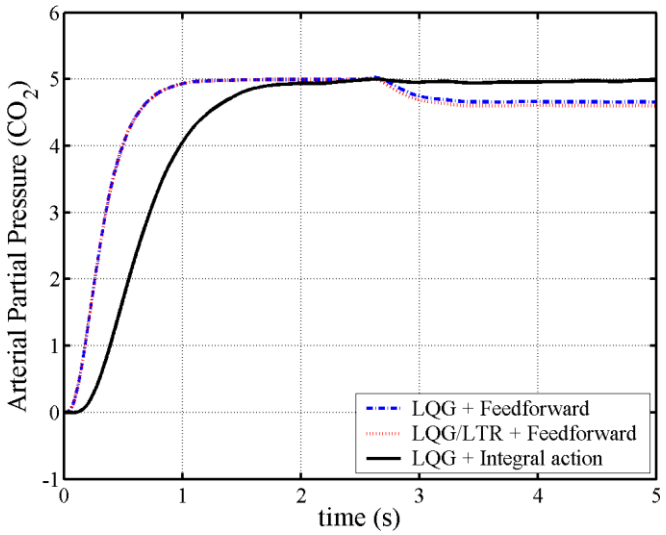

Fig. 9: Step response of CO_2 arterial partial pressure

Table 3

	LQG + Feedforward	LQG/LTR + Feedforward	LQG + Integral
Bandwidth (Hz) (CO_2 flow rate)	≈ 5	≈ 5.15	≈ 0.85
Bandwidth (Hz) (O_2 flow rate)	∞	∞	≈ 1.9

From Table (3) it can be clearly noticed that the LQG and LQG/LTR with feedforward control have much higher bandwith requirements than the LQG with integral control. This difference is even more pronounced for the O_2 flow rate where only the bandwidth for the LQG with integral control can be physically realized.

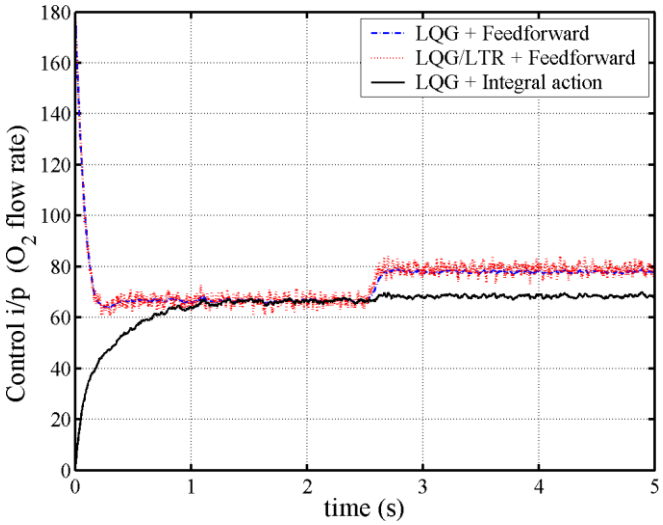

Fig. 10: Controller output in O_2 flow rate

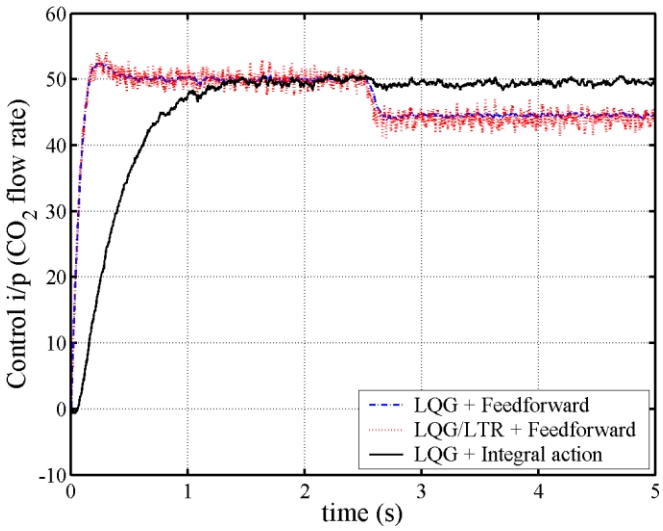

Fig. 11: Controller output in CO_2 flow rate

Fig. 12 shows the structured singular values for the parametric uncertainty being considered in (22) and (23). As mentioned earlier, all the controllers were designed so as to ensure that the robust stability condition given by (24) is satisfied. However, it is interesting to notice that the LQG/LTR control slightly reduces the robust stability characteristic of the system compared to the LQG by itself. In Fig. 12, only two out of the four structured singular values have been plotted, since the other two values are close to zero due to the nature of the perturbation. It can be clearly seen from the figure that although addition of integral action reduces the degree of robustness, it still satisfies the robust stability criteria of (24).

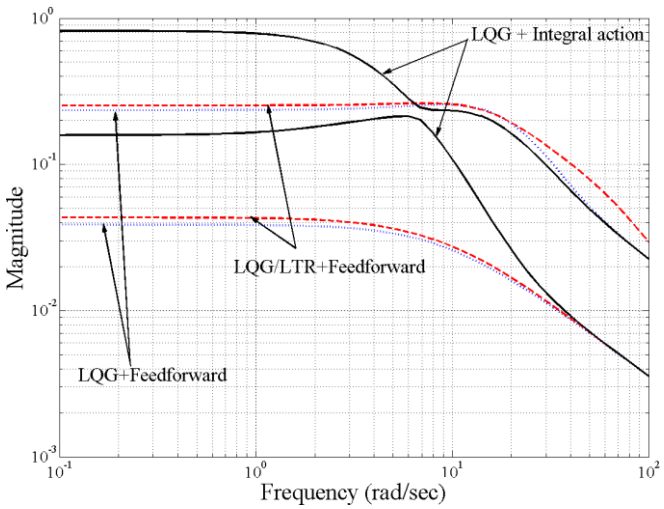

Fig. 12: Structured singular value analysis

VI. Conclusion

The paper investigated three different types of LQG based controllers designed for tracking control of the arterial partial pressures of the blood gases (O_2 and CO_2) during a typical ECMO procedure. The system included a membrane oxygenator for introducing the above mentioned gases into the bloodstream and a blood gas sensor for measuring their resulting arterial partial pressures in the blood. The performance of each of the controllers was ascertained both from a tracking as well as disturbance rejection standpoint to step commands in both these inputs. Robustness analysis was also performed on all the closed loop configurations using the structured singular value analysis and the performance of all the controllers was tuned so as to ensure robust stability to the parametric uncertainties considered. While the LQG and LQG/LTR with feed forward control were able to achieve good tracking performance, only the LQG augmented with integral control was able to achieve accurate tracking of the arterial partial pressures of the blood gases in the presence of a step input disturbance in the blood gases flow rates. It was also noticed that the LQG augmented with integral control required lesser bandwidth to achieve the better performance. Extension to this work will involve investigation of H_∞ based control schemes for comparison with the optimal control methodologies designed in this paper.

References

[1] J. B. Burl, "Linear Optimal Control H_2 and H_∞ Methods," 1999, Addison Wesley Longman, Inc.

[2] Extracorporeal Circulation Terms and Definitions. *Medical Glossary*. [Online] [Cited: August, 2010.] Available: http://www.medicalglossary.org/surgical_procedures_operative_extracorporeal_circulation_definitions.html.

[3] M. Drummond, "Technological Evolution of Membrane Oxygenators," April, 2005, Revista Brasileira de Cirurgia Cardiovascular, Vol. 20, pp. 432-467.

[4] K. Maier, What is an ECMO machine? *wiseGEEK*. [Online] [Cited: August 25, 2010.] http://www.wisegeek.com/what-is-an-ecmo-machine.htm.